

AD _____

GRANT NUMBER DAMD17-94-J-4368

TITLE: pH Regulation by Breast Cancer Cells in Vitro and in Vivo

PRINCIPAL INVESTIGATOR: Robert J. Gillies, Ph.D.

CONTRACTING ORGANIZATION: University of Arizona
Tucson, Arizona 85719

REPORT DATE: September 1996

TYPE OF REPORT: Annual

PREPARED FOR: Commander
U.S. Army Medical Research and Materiel Command
Fort Detrick, Frederick, Maryland 21702-5012

DISTRIBUTION STATEMENT: Approved for public release;
distribution unlimited

The views, opinions and/or findings contained in this report are those of the author(s) and should not be construed as an official Department of the Army position, policy or decision unless so designated by other documentation.

19970117 105

1

REPORT DOCUMENTATION PAGE

Form Approved
OMB No. 0704-0188

Public reporting burden for this collection of information is estimated to average 1 hour per response, including the time for reviewing instructions, searching existing data sources, gathering and maintaining the data needed, and completing and reviewing the collection of information. Send comments regarding this burden estimate or any other aspect of this collection of information, including suggestions for reducing this burden, to Washington Headquarters Services, Directorate for Information Operations and Reports, 1215 Jefferson Davis Highway, Suite 1204, Arlington, VA 22202-4302, and to the Office of Management and Budget, Paperwork Reduction Project (0704-0188), Washington, DC 20503.

1. AGENCY USE ONLY (Leave blank)		2. REPORT DATE September 1996	3. REPORT TYPE AND DATES COVERED Annual (15 Aug 95 - 14 Aug 96)	
4. TITLE AND SUBTITLE pH Regulation by Breast Cancer Cells in Vitro and Vivo			5. FUNDING NUMBERS DAMD17-94-J-4368	
6. AUTHOR(S) Robert J. Gillies, Ph.D.				
7. PERFORMING ORGANIZATION NAME(S) AND ADDRESS(ES) University of Arizona Tucson, Arizona 85719			8. PERFORMING ORGANIZATION REPORT NUMBER	
9. SPONSORING/MONITORING AGENCY NAME(S) AND ADDRESS(ES) Commander U.S. Army Medical Research and Materiel Command Fort Detrick, Frederick, Maryland 21702-5012			10. SPONSORING/MONITORING AGENCY REPORT NUMBER	
11. SUPPLEMENTARY NOTES				
12a. DISTRIBUTION / AVAILABILITY STATEMENT Approved for public release; distribution unlimited			12b. DISTRIBUTION CODE	
13. ABSTRACT (Maximum 200) <p>The pH of tumors plays an important role in therapeutic efficacy, and may have relevance to carcinogenesis itself. A technique has been developed to simultaneously measure the extracellular pH (pHe) and the intracellular pH (pHi) of tumors in vivo using <i>in vivo</i> Magnetic Resonance Spectroscopy (MRS). During the past year, this technique has been refined to accurately report the pHe distribution within the tumor. This is significant since at the low extremes therapy using weakly basic chemotherapeutic agents, such as doxorubicin, is significantly hindered.</p> <p>A quantitative model has demonstrated that the turnover of acidic vesicles within cells can also contribute to cellular resistance to weakly basic chemotherapeutic drugs. During the past year, this model has been developed and measurements of acidic vesicle turnover have begun. Drug resistant MCF/7 cell variants have a higher rate of vesicle turnover rate than do their drug-sensitive counterparts. Furthermore, they express a plasma membrane activity of vacuolar-type H(+) ATPases (V-ATPases) which may be a consequence of this vesicle turnover.</p> <p>In order to quantify the turnover of these V-ATPase containing vesicles, antibodies against an extracellular epitope of the pump are required. Only the 115 kDa subunit exposes an extracellular epitope and, during the past year, the human sequence of the 115 kDa subunit has been cloned and sequenced. This subunit exhibits alternative splicing such as that observed previously in the bovine 115 kDa subunit.</p>				
14. SUBJECT TERMS Breast Cancer			15. NUMBER OF PAGES 17	
			16. PRICE CODE	
17. SECURITY CLASSIFICATION OF REPORT Unclassified	18. SECURITY CLASSIFICATION OF THIS PAGE Unclassified	19. SECURITY CLASSIFICATION OF ABSTRACT Unclassified	20. LIMITATION OF ABSTRACT Unlimited	

FOREWORD

Opinions, interpretations, conclusions and recommendations are those of the author and are not necessarily endorsed by the US Army.

Pg Where copyrighted material is quoted, permission has been obtained to use such material.

Pg Where material from documents designated for limited distribution is quoted, permission has been obtained to use the material.

Pg Citations of commercial organizations and trade names in this report do not constitute an official Department of Army endorsement or approval of the products or services of these organizations.

Pg In conducting research using animals, the investigator(s) adhered to the "Guide for the Care and Use of Laboratory Animals," prepared by the Committee on Care and Use of Laboratory Animals of the Institute of Laboratory Resources, National Research Council (NIH Publication No. 86-23, Revised 1985).

Pg For the protection of human subjects, the investigator(s) adhered to policies of applicable Federal Law 45 CFR 46.

Pg In conducting research utilizing recombinant DNA technology, the investigator(s) adhered to current guidelines promulgated by the National Institutes of Health.

Pg In the conduct of research utilizing recombinant DNA, the investigator(s) adhered to the NIH Guidelines for Research Involving Recombinant DNA Molecules.

Pg In the conduct of research involving hazardous organisms, the investigator(s) adhered to the CDC-NIH Guide for Biosafety in Microbiological and Biomedical Laboratories.

Peter J. Lee
PI - Signature

9/30/96
Date

Table of Contents

Page

1	Introduction
	Body
1	Measurement of intracellular and extracellular pH of tumors <i>in vivo</i>
8	H ⁺ -ATPase and Multidrug Resistance
9	Cloning of 115 kDa Subunit of Human Vacuolar-type H ⁺ -ATPase
11	Relationship to original Statement of Work
11	Conclusions
12	References

INTRODUCTION

The pH of tumors plays an important role in the efficacy of chemotherapy and radiotherapy, and may have relevance to carcinogenesis itself. A technique has been developed to simultaneously measure the extracellular pH (pHe) and the intracellular pH (pHi) of tumors *in vivo* using magnetic Resonance Spectroscopy (MRS). During the past year, this technique has been refined to accurately report the entire pHe distribution within the tumor. This is significant since, at the low extremes, acidic pH has been reported to be mutagenic and clastogenic. Furthermore, design of therapy using weakly basic chemotherapeutic agents, such as doxorubicin, requires accurate knowledge of the pH range. Resistance to weakly basic chemotherapeutic drugs (WBDR) can be augmented by acidic pHe. Furthermore, a quantitative model has demonstrated that the turnover of acidic vesicles within cells can also contribute to WBDR. During the past year, this model has been developed and measurements of acidic vesicle turnover have begun. Drug resistant MCF/7 cell variants have a higher rate of vesicle turnover than do their drug sensitive parental lines. Furthermore, they express a plasma membrane activity of vacuolar-type H(+) ATPases (V-ATPases) which may be a consequence of this vesicle turnover. In order to quantify the turnover of these V-ATPase containing vesicles, antibodies against an extracellular epitope of the pump are required. Only the 115 kDa subunit exposes an extracellular epitope and, during the past year, the human sequence of the 115 kDa subunit has been cloned and sequenced. Furthermore, this subunit exhibits alternative splicing such as that observed previously in the bovine 115 kDa subunit. With regard to the original Statement of Work, the above projects are proceeding ahead of schedule, whereas the fluorescence-based experiments have been postponed until next year.

BODY

Project 1. Measurement of intracellular and extracellular pH of tumors *in vivo*.

Introduction. Extracellular pH in tumors has been found to have a bearing on the effectiveness of different treatment strategies. Increasing tumor acidity increases thermal sensitivity of tumors and may also play a role in the effectiveness of chemotherapeutic agents, many of which are weak bases (Tannock and Rotin, 1989). The partition of weak base molecules across the cell membrane is dependent on intra- and extracellular pH. Knowledge of pH distribution within tumors thus has clinical relevance. The chemical shift of the ^{31}P nucleus in 3-aminopropylphosphonate (3-APP), a cell-impermeant molecule, is pH-sensitive, making it a good indicator of extracellular pH (Gillies et al., 1994). A robust calibration equation for the chemical shift of 3-APP has been reported earlier by us which can be used to calculate the pH distribution *in vivo*. However, the lineshape of the 3-APP peak is dependent not just on the pH distribution within the sample, but is also broadened by T_2^* effects. In our previous work, we used ^{31}P spectra from tumors in animals euthanatized within the magnet to deconvolve T_2^* effects from the 3-APP peak obtained

from the live animal. That technique required acquisition of several ^{31}P spectra following death. We have since developed a new deconvolution technique which only requires one ^{31}P and one ^1H spectrum, both from the live animal.

Tumors Used. Mitoxantrone-resistant MCF-7 human breast carcinoma cells were implanted in the mammary fat pads of 6-8 week old female SCID mice; 1×10^6 cells were inoculated subcutaneously in 0.05 mL of Hank's balanced salt solution. Tumors were allowed to grow for 6-8 weeks to volumes of 700-1200 mm^3 , as estimated by external measurements of three orthogonal dimensions of the tumor. Mice were anesthetized with a combination of ketamine (72 mg/kg), xylazine (6 mg/kg) and acepromazine (6 mg/kg). 3-aminopropylphosphonate (3APP, 0.15-0.3 mL, 128 mg/mL, pH 7.3) was administered at the appropriate time via an i.p. catheter. Spectra were acquired before and after administration of 3APP without moving the animal.

T_1/T_2 Measurements. The T_1 and T_2 relaxation times of 3APP were measured *in vitro* at 37°C on a Bruker AMX 400 at 9.4 T in two solutions, phosphate-buffered saline and fetal bovine serum. In addition, they were also measured at 4.7 T on a Bruker Biospec in an excised tumor. The tumor was soaked in 3APP (400 mM, pH 7.4) for 2 hours prior to spectroscopy.

***In vivo* ^1H and ^{31}P NMRS Measurements.** All *in vivo* measurements were performed at 4.7 T using a solenoid coil tunable to ^1H or ^{31}P . ^{31}P spectra were acquired using 10° pulses and recycle times of 200-500 ms. ^1H spectra were acquired either using a spin-echo sequence with water-presaturation, or by double quantum coherence transfer (DQCT) (Hurd and Freeman, 1991; Mason et al., 1993). For the spin-echo spectra, a TE of 240 ms was found to be optimal. With the DQCT sequence, it was necessary to average 2048 scans (≈ 40 min) for sufficient signal-to-noise ratios.

Deconvolution Theory. The pH-sensitive ^{31}P NMRS resonance of 3APP from a tumor will be broadened by the pH-heterogeneity within the tumor. In addition, the resonance will also be broadened by magnetic field heterogeneities across the tumor, and by spin-spin relaxation effects: together, these two factors may be combined into one, the T_2^* effect. In order to assess the pH-heterogeneity within the tumor from the shape of the *in vivo* 3APP resonance, we need to deconvolve the contribution of the T_2^* effects to the 3APP peak.

An FID, described by the function $\exp(-t/T_2^*)$ may be multiplied by a gaussian function $\exp\{-(t-\tau)^2/[2\sigma^2]\}$ to yield:

$$\exp\{-t^2/(2\sigma^2)\} \cdot \exp\{-\tau^2/(2\sigma^2)\} \cdot \exp\{t/(\sigma^2/\tau) - t/T_2^*\}$$

where τ and σ are the offset and standard deviation of the distribution. If σ and τ are chosen such that $\sigma^2/\tau = T_2^*$, the FID is transformed into the function:

$$\exp\{-t^2/(2\sigma^2)\} \cdot \exp\{-\tau^2/(2\sigma^2)\},$$

which is no longer dependent on T_2^* . Thus, the resonance now has a width reflecting only the pH heterogeneity within the sample.

In order to achieve this deconvolution, we require knowledge of the effective T_2^* of the ^{31}P nuclei of 3-APP molecules within the sample. Titrations of 3-APP in the pH range 6.6-7.4 reveal that the chemical shift of the protons on the γ -carbon of 3-APP is pH-insensitive and is at 3.06 ppm. The linewidth of this resonance can be used to estimate the magnetic field heterogeneity impinging on the 3-APP molecules as follows:

For the ^1H nuclei on the γ -carbon in 3-APP:

$$1/T_{2,1\text{H}}^* = 1/T_{2,1\text{H}} + 1/T_{2,1\text{H}}^*,$$

where $1/T_{2,1\text{H}}^*$ arises from heterogeneity in the B_0 field. For the ^{31}P nucleus in 3-APP:

$$1/T_{2,31\text{P}}^* = 1/T_{2,31\text{P}} + (1/T_{2,1\text{H}}^*) \cdot (\gamma_{31\text{P}}/\gamma_{1\text{H}}).$$

This equation gives the desired $T_{2,31\text{P}}^*$.

$T_{2,1\text{H}}$ and $T_{2,31\text{P}}$ were obtained from measurements made on an excised tumor, as explained earlier. $T_{2,1\text{H}}^*$ was obtained for each tumor from a spin-echo or DQCT ^1H NMRS spectrum of the tumor. In the former case, spectra were acquired from tumors prior to injection of the 3APP, and 30 minutes after the 3APP was delivered. The difference of these two spectra permitted the 3APP peak at 3.06 ppm to be resolved despite interference from the choline peak at 3.1 ppm (figure 2). DQCT ^1H spectra were directly used to estimate $T_{2,1\text{H}}^*$ as the linewidth of the γ -CH₂ proton peak at 3.06 ppm.

RESULTS

T_1 and T_2 measurements

The values of the T_1 and T_2 relaxation times for the ^1H and ^{31}P nuclei in 3APP measured under various conditions are listed in tables 1-3. The T_1 and T_2 relaxation times of the nuclei in 3APP were first measured at a magnetic field strength of 9.4T in two solutions, fetal bovine serum and phosphate-buffered saline, in order to assess the influence of the chemical environment on the relaxation times. It can be seen from tables 1 and 2 that the values of the T_1 and T_2 relaxation times of the ^1H and ^{31}P nuclei in 3APP are significantly affected by the nature of the chemical environment (the solution) surrounding the nuclei. Our deconvolution technique requires that we measure the T_2 of the ^1H nuclei on the γ -carbon in 3-APP under conditions closely mimicking the *in vivo* milieu. The relatively low

in vivo concentration of 3APP precluded the direct measurement of T_1 and T_2 in the living animal. Therefore, an excised tumor which had been soaked in a 400mM solution of 3APP (pH 7.4) for 2 hours prior to spectroscopy was used as a "phantom". The measurements were made at 37°C.

Table 1. T_1 of 3-aminopropylphosphonate (9.4T, 37°C).

Nucleus	T_1 (PBS*)	T_1 (FBS#)
$^1\text{H}_{\text{C}3}$, 3.06 ppm	1.17 ± 0.06 s	1.08 ± 0.07 s
$^1\text{H}_{\text{C}2}$, 1.95 ppm	1.0 ± 0.05 s	0.93 ± 0.06 s
$^1\text{H}_{\text{C}1}$, 1.60 ppm	0.90 ± 0.04 s	0.83 ± 0.04 s
^{31}P	3.51 ± 0.13 s	3.42 ± 0.16 s

*: phosphate-buffered saline, pH 7.4

#: fetal bovine serum, pH 7.4

Table 2. T_2 of 3-aminopropylphosphonate (9.4T, 37°C).

Nucleus	T_2 (PBS*)	T_2 (FBS#)
$^1\text{H}_{\text{C}3}$, 3.06 ppm	0.79 ± 0.07 s	0.57 ± 0.06 s
$^1\text{H}_{\text{C}2}$, 1.95 ppm	0.67 ± 0.07 s	0.51 ± 0.05 s
$^1\text{H}_{\text{C}1}$, 1.60 ppm	0.58 ± 0.06 s	0.46 ± 0.04 s
^{31}P	2.3 ± 0.2 s	1.7 ± 0.2 s

*: phosphate-buffered saline, pH 7.4

#: fetal bovine serum, pH 7.4

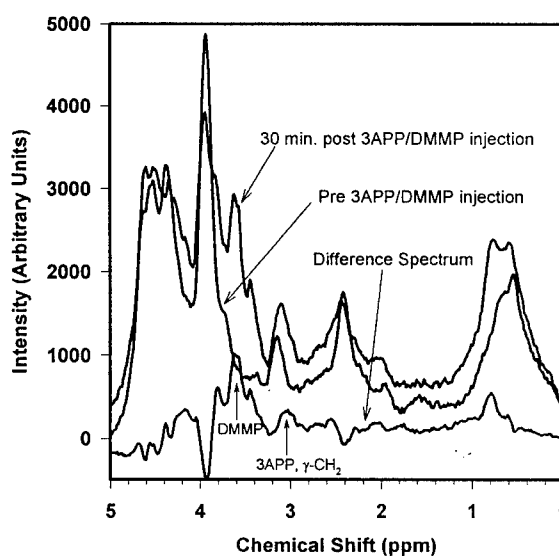
Table 3. T_1 and T_2 of 3-aminopropylphosphonate in Excised Tumor (4.7T, 37°C). These values were used in the deconvolution.

Nucleus	T_1	T_2
$^1\text{H}_{\text{C3}}$, 3.06 ppm	0.52 ± 0.05 s	112 ± 11 ms
$^1\text{H}_{\text{C2}}$, 1.95 ppm	0.47 ± 0.04 s	96 ± 10 ms
$^1\text{H}_{\text{C1}}$, 1.60 ppm	0.41 ± 0.04 s	84 ± 9 ms
^{31}P	1.9 ± 0.1 s	0.42 ± 0.04 s

^1H and ^{31}P Spectroscopy

Spin-Echo ^1H NMRS. Figure 1 shows spin-echo spectra acquired before and after the injection of 3APP (and DMMP, in some cases) into a SCID mouse. In some cases, the 3APP resonance at 3.06 ppm in the difference spectrum was resolved well enough to permit the estimation of $T_{2,1\text{H}}^*$ for use in the deconvolution.

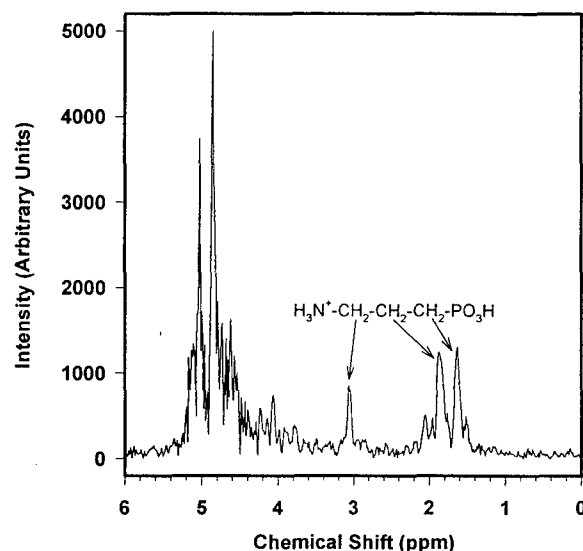
Figure 1. *In vivo* Spin-Echo ^1H MRS Spectrum of a MCF-7/Mitox tumor. TE = 240 ms.



DQCT ^1H Spectroscopy. In many cases, the 3APP resonance at 3.06 ppm in a difference spectrum such as shown in figure 1 was not sufficiently resolved from the background to permit the estimation of $T_{2,1\text{H}}^*$. Figure 2 shows an *in vivo* Double Quantum Coherence Transfer (3,4) ^1H spectrum of 3APP in a tumor. Although DQCT results in increased times to obtain acceptable signal-to-noise ratios, the absence of interfering resonances in the

3.1 ppm region facilitated the estimation of $T_{2,1H}^*$ from the 3APP resonance at 3.06 ppm.

Figure 2. *In vivo* Double Quantum Coherence Transfer 1H Spectrum of 3-aminopropylphosphonate from a MCF-7/Mitox tumor. The linewidth of the 3APP resonance at 3.06 ppm was used to estimate $T_{2,1H}^*$.



^{31}P NMRS. Figure 3 shows an *in vivo* ^{31}P NMRS spectrum, as well as the result from the deconvolution of $T_{2,31P}^*$ from the linewidth of the 3APP resonance. The inset in figure 3 shows the pH_{ex} distribution for this tumor obtained by converting the lineshape of the deconvolved 3APP resonance to pH values using the titration equation:

$$pH = 6.91 + \log_{10} \left(\frac{\delta_{3APP} - 21.1}{24.3 - \delta_{3APP}} \right) \quad (1)$$

In addition, the intensity at any point on the pH distribution was corrected by dividing by the slope of equation 1, as per the method of Graham et al. (Graham et al., 1994).

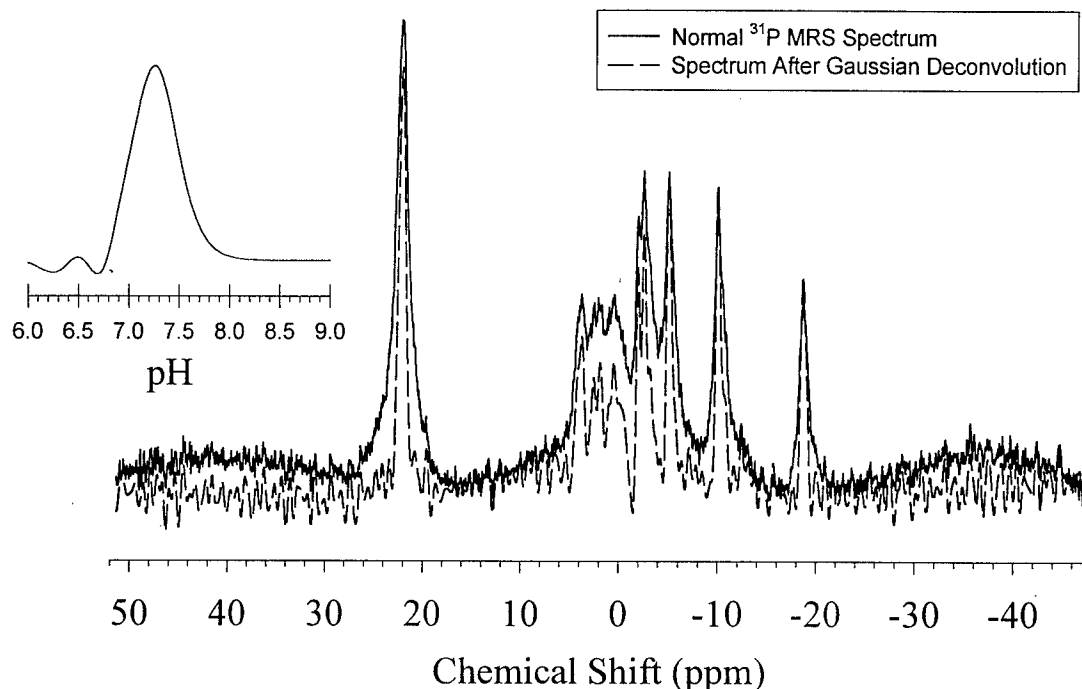
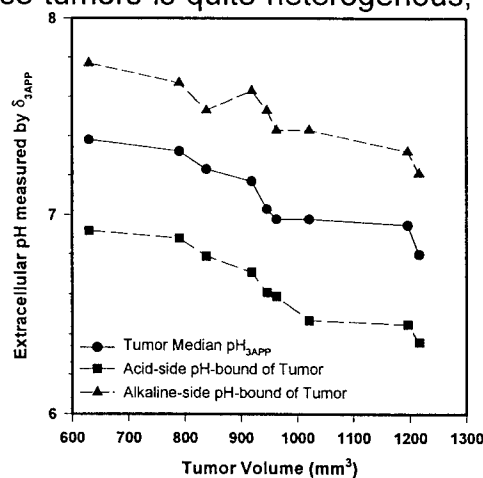


Figure 3. Extracellular pH distribution in a MCF-7/Mitox tumor grown in a SCID mouse.

Variation in tumor pH with tumor volume

It is clear from figure 3 that the deconvolution has accomplished a substantial narrowing of the 3APP resonance. Rigorous error propagation analyses are underway to investigate the effect of errors in T_2 values on the calculated range of extracellular pH within the tumor. In addition to the median tumor pH values, figure 4 shows the range of extracellular pH excursions in the tumor, calculated from the bounds of the deconvolved 3APP peak. It can be seen that the extracellular pH within these tumors is quite heterogenous, and varies over a range of 0.8-1.0 pH units.

Figure 4. Range of extracellular pH variation within a MCF-7/Mitox tumor.



Project 2. H⁺-ATPase and Multidrug Resistance.

A major barrier to successful chemotherapeutic treatment of cancer is the development of drug resistance by cells in tumors. Cells acquiring resistance to one type of drug almost always show resistance to other chemically unrelated drugs. Hence, the phenomenon is known as multidrug resistance (MDR). The most well-studied mechanism of multidrug resistance involves the MDR-1 gene product, P-glycoprotein (P-gp), a drug pump which also transports protons (Thiebaut et al., 1990; Boscoboinik et al., 1990). However, P-gp accounts for only 50% of the observed MDR phenotypes (Gottesman and Pastan, 1993). Tumor pH can contribute to the resistance to weakly basic drugs, and this can be attributed to the phenomenon of "ion trapping", wherein the drugs are accumulated in acidic compartments and excluded from alkaline compartments (Tannock and Rotin, 1989; Jahde et al., 1990; Roepe et al., 1993; Simon et al., 1994). Weakly basic drug resistance (WBDR) is not classically MDR, since the drugs are structurally related. However WBDR is clinically important since weak base chemotherapeutic drugs, such as mitoxantrone and doxorubicin (adriamycin), are commonly used to treat cancer.

Ion trapping is relevant to WBDR not only because of the acidic tumor environment (see above), but also by sequestration of drugs into acidic vesicles. Intracellular compartments are acidified through the action of V-ATPases, and there is considerable evidence that these pumps can be involved in multidrug resistance. Sehested et al. (1987) observed enhanced rates of exocytosis in multidrug resistant EAT cells, compared to their drug-sensitive counterparts. Dubowchik et al. (1994) have shown that lysosomotropic weak bases raise intravesicular pH as well as reverse doxorubicin resistance in NCT116-VM46 colon carcinoma cells. Similar results were presented by Sehested et al. (1988).

We have investigated the role of pH in WBDR using a cell line, MCF/7-mitox, which displays an MDR phenotype, yet does not possess P-gp (Taylor et al., 1991). MCF/7-mitox cells treated with mitoxantrone sequester it into subcellular vesicles (Willingham et al., 1986). We hypothesize that overexpressed pmV-ATPases may be involved in the MDR phenotype of these cells (e.g. Marquardt and Center, 1991). Both MCF/7-mitox as well as P-gp-positive MCF/7-dox cells contain pmV-ATPase activity, while parental MCF/7 cells do not (Fig. 5a). Furthermore, growth of parental MCF/7 cells at acid pH induces pmV-ATPase activity and drug resistance (Fig. 5b). We have also begun to investigate the synergy between weak bases and V-ATPase inhibitor in disrupting vesicular pH gradients. In MCF/7 cells, 840 nM bafilomycin is needed to alkalinize endosomes half-maximally (IC₅₀). In the presence of 5 mM NH₄Cl, 400 nM bafilomycin is sufficient to completely collapse the endosomal pH gradient. Thus the effects of weak bases and V-ATPase inhibitors are additive or synergistic.

We have written a manuscript which details the effect of acidic vesicle recycling on resistance to common, weakly basic chemotherapeutic drugs, such as mitoxantrone and doxorubicin (adriamycin). Using conservative estimates for parameters of vesicle size,

number, pH and turnover rate, it can be clearly demonstrated that 1) vesicle movement contributes greatly to a multidrug-resistant phenotype, 2) activity of drug pumps (i.e. P-gp) that are statically resident on the plasma membrane would be insufficient to confer drug resistance, and 3) the activity of V-ATPase combined with a drug/H⁺ exchange activity would be kinetically identical to the activity of p-glycoprotein.

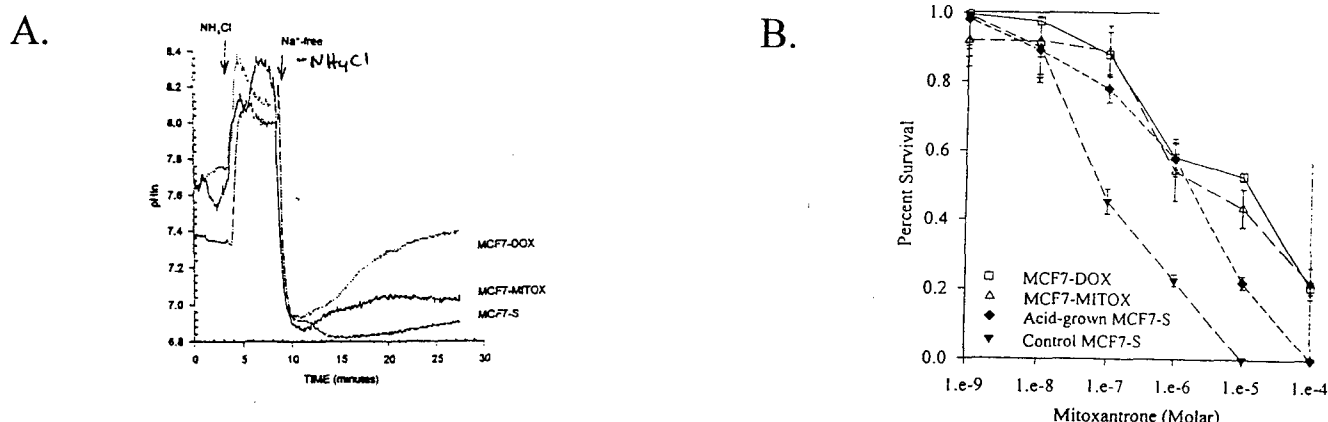


Figure 5. pmV-ATPase and drug resistance. (A) pmV-ATPase activity in MCF/7, MCF/7-mitox and MCF/7-dox cells. Cells were acidified with a pre-pulse of NH₄Cl and then perfused with buffer at pH 8.0 lacking Na⁺- and HCO₃⁻. Recovery is due to pmV-ATPase and is inhibitable with bafilomycin. (B) Survival of MCF/7 cells following 48 hours in the presence of mitoxantrone. Cells used were MCF/7-S, MCF/7-mitox, MCF/7-dox, and MCF/7-S cells acclimated to low pH.

Project 3. Cloning of 115 kDa Subunit of Human Vacuolar-type H⁺-ATPase.

The involvement of acidic vesicles in drug resistance requires that they recycle rapidly to the plasma membrane. From our work, we believe that these vesicles contain vacuolar-type H(+)-ATPases (V-ATPases), large multimeric proteins generally found in intracellular vesicles and in the plasma membranes of tumor cells. In order to measure this turnover, antibodies are required which recognize an extracellular epitope of this pump. The only subunit which presents an extracellular epitope is the 115 kDa subunit. Prior to this work, the sequence of the human 115 protein was not known. We have generated a complete sequence of this protein by screening a pancreatic library with a probe from the bovine sequence.

Methods and Results. A fragment of the bovine 116 kDa subunit in bluescript vector was obtained from Dennis Stone. From this a 1200 b.p. fragment was excised, 5' 32-P end-labeled and used to screen a human pancreatic cDNA library. Twelve positive colonies were identified, subsequently sub-cloned into pBS and sequenced by the dideoxy chain

termination method. Overlapping clones were identified as contigs, and the full length sequence was identified (GenBank accession number L78933, available Oct. 1996). The resulting nucleic acid sequence has >90% identity to the bovine sequence. An open reading frame of >3000 bp was identified and the putative translation product shares 97% and 95% identity at the amino acid level to the previously reported bovine and rat sequences, respectively (Fig. 6A). Our clone has <50% identity to a previously reported human osteoclast-specific cDNA clone, although the hydropathy plots are highly homologous. Because Stone had previously reported alternative splicing for the bovine 116 kDa subunit, we designed PCR primers to flank this region at nucleotide 2106. PCR was performed on 28 human cDNA libraries. All non-neuronal libraries yielded only a single product at the predicted molecular weight, whereas 6/9 neuronal libraries yielded three PCR products (Fig. 6B). These are currently being sequenced to determine the identity of these additional sequences. *Additional work using this sequence will be undertaken by Charles Fehr under the auspices of his USAMRAA pre-doctoral award DAMD17-96-1-6188.*

**Amino Acid Sequence Comparison
Human vs. Bovine**

116kDa: 115 kD V-ATPase subunit (801 a.a.)
216kDa: 115 kD V-ATPase subunit (818 a.a.)

Human	NCLEFASKEKTLADFLQSEAAVCCVSELCGLQAV
Bovine	NCLEFASKEKTLADFLQSEAAVCCVSELCGLQAV
Human	QFADLPDVMVVFQAKTVNEVARCEKDRLELFFVEX
Bovine	QFADLPDVMVVFQAKTVNEVARCEKDRLELFFVEX
Human	ICRKAWIFINOTQENFVVFPRDXIDLEAMFETIE
Bovine	ICRKAWIFINOTQENFVVFPRDXIDLEAMFETIE
Human	HELKEINTHQAALRNFLLELTELFLAKTQGVFD
Bovine	HELKEINTHQAALRNFLLELTELFLAKTQGVFD
Human	ENADFDLLEKESLLEPSENGACQFLPLQGVVAVI
Bovine	ENADFDLLEKESLLEPSENGACQFLPLQGVVAVI
Human	RRKIIPTFELHNVCCGVFLQAGAESFPLEDPV
Bovine	RRKIIPTFELHNVCCGVFLQAGAESFPLEDPV
Human	TCGVNKSVFIFFGDDLEKRVKRICQFRAELY
Bovine	TCGVNKSVFIFFGDDLEKRVKRICQFRAELY
Human	PCPTTQEKKEKACGVNTHIDDLQVLMQTEDRRO
Bovine	PCPTTQEKKEKACGVNTHIDDLQVLMQTEDRRO
Human	RVLQAAAKNIRVMFIRVKNKAITHTLCLCVIDVT
Bovine	RVLQAAAKNIRVMFIRVKNKAITHTLCLCVIDVT
Human	QKCLIAEVVCPVTDLQSLQFALKRGTEKSGTVFS
Bovine	QKCLIAEVVCPVTDLQSLQFALKRGTEKSGTVFS
Human	ILNRRQTMOTFTYKNTNFTYGVQFQVDAVGIGT
Bovine	ILNRRQTMOTFTYKNTNFTYGVQFQVDAVGIGT
Human	VREINPAPYTIITZFFFLFAVNFQDENGILMTLFA
Bovine	VREINPAPYTIITZFFFLFAVNFQDENGILMTLFA
Human	VNVVVLSSSLQGEKHEKNTFTYGRVITILLNGV
Bovine	VNVVVLSSSLQGEKHEKNTFTYGRVITILLNGV
Human	FTTGLITNDQFSEKSLNIFGSSMVSVPNFVNM
Bovine	FTTGLITNDQFSEKSLNIFGSSMVSVPNFVNM
Human	TEETLKGNFVLLQMPFCVFCGYPFFCDDPIKNI
Bovine	TEETLKGNFVLLQMPFCVFCGYPFFCDDPIKNI
Human	ATRELTFLNFFNKNRNVLCGILNHLFGVSLFVFN
Bovine	ATRELTFLNFFNKNRNVLCGILNHLFGVSLFVFN
Human	TFKXFLNIVFCFIPFIFHTLFGVCLVILFVFN
Bovine	TFKXFLNIVFCFIPFIFHTLFGVCLVILFVFN
Human	TAVAKTSAPSLINFINNPLFESQENY
Bovine	TAVAKTSAPSLINFINNPLFESQENY
Human	SGQEDICQFLVVVALLCVFNNLLFPLVLRAGYLA
Bovine	SGQEDICQFLVVVALLCVFNNLLFPLVLRAGYLA
Human	RENHGLTFGGINVGNQPTFEDAKIIONDQLETRN
Bovine	RENHGLTFGGINVGNQPTFEDAKIIONDQLETRN
Human	EDAKIIONDQLETRN
Bovine	EDAKIIONDQLETRN
Human	TASTLRLMALALAAHEVLMTHVIRIGLVKSL
Bovine	TASTLRLMALALAAHEVLMTHVIRIGLVKSL
Human	ADGLTFPATITVAILLIMEGLSAFLVALA
Bovine	ADGLTFPATITVAILLIMEGLSAFLVALA
Human	LEWVEFGHFFVSGTGFPLFPFENIRACK
Bovine	LEWVEFGHFFVSGTGFPLFPFENIRACK

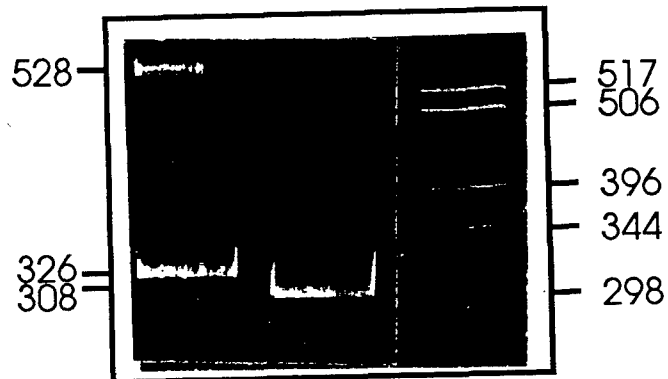


Figure 6A. Predicted amino acid sequences of human and bovine 116 kDa subunits (differences shaded).

Figure 6B. Ethidium bromide stained 5% non-denaturing PAGE gel of PCR products from hippocampal (lane 1) and pancreatic (lane 2) cDNA libraries.

RELATIONSHIP TO ORIGINAL STATEMENT OF WORK

Task 1a, measurement of intracellular and extracellular pH by fluorescence in complete buffer, using all four cell lines, was completed, as per our previous report. A manuscript describing our results is in preparation.

Task 1b, Titrations of two cell lines using MRS of cells cultured in bioreactors was postponed to year 04 due to late availability of suitable bioreactors.

Task 1c and 1d, analysis of data, were postponed pending completion of task 1b.

Tasks 2a-d, determination of pH regulatory mechanisms, have been partially completed. Data analysis has been slowed due to non-availability of a technician. We anticipate completing these tasks in year 04.

Tasks 3a-d, experiments on measurement of tumor pH as a function of tumor size *in vivo*, are proceeding ahead of schedule. We have completed the pH studies for one cell line, and analysis of data on proliferative fractions in these tumors is ongoing. A manuscript describing our results is also being written. Measurements for other cell lines, as well as experiments on variation of tumor blood flow with tumor size will be completed in year 03.

Tasks 4a-b, effects of altering blood flow on extracellular and intracellular pH, and analysis of data, will be completed in year 03.

CONCLUSIONS

- T_2^* deconvolution of 3APP resonances *in vivo* can be used to effectively determine the extracellular pH distribution in transplanted mammary tumors.
- The extracellular pH of tumors decreases with increasing tumor size.
- Turnover of acidic vesicles can significantly augment resistance of cells to weakly basic chemotherapeutic drugs, such as mitoxantrone and doxorubicin.
- Drug-resistant MCF/7 variants have higher rates of vesicle turnover than do their drug-sensitive counterparts.
- The cDNA for the human 115 kDa subunit of the vacuolar-type H(+) ATPase has been identified and sequenced. PCR of this gene from different libraries suggests that it is alternatively spliced in neuronal cells.

REFERENCES

- Boscoboinik D, Gupta RS and Epand RM (1990) Investigation of the relationship between altered intracellular pH and multidrug resistance in mammalian cells, *Br. J. Cancer* **61**: 568-572.
- Dubowchik GM, Padilla L, Edinger K and Firestone RA (1994) Reversal of doxorubicin resistance and catalytic neutralization of lysosomes by a lipophilic imidazole, *Biochim. Biophys. Acta* **1191**: 103-108.
- Gillies RJ, Liu Z and Bhujwala Z (1994) ^{31}P -MRS measurements of extracellular pH of tumors using 3-aminopropylphosphonate, *Am. J. Physiol.* **267**: C195-C203.
- Gotessman MM and Pastan I (1993) Biochemistry of multidrug resistance mediated by the multidrug transporter, *Ann. Rev. Biochem.* **62**: 385-427.
- Graham RA, Taylor AH and Brown TR (1994) A method for calculating the distribution of pH in tissues and a new source of pH error from the ^{31}P -NMR spectrum, *Am. J. Physiol.* **266**: R638-R645.
- Hurd RE, and Freeman D (1991) Proton editing and imaging of lactate, *NMR in Biomed.* **4**: 73-80.
- Jahde E, Glusenkamp KH and Rajewsky MF (1990) Protection of cultured malignant cells from mitoxantrone cytotoxicity by low extracellular pH: a possible mechanism for chemoresistance *in vivo*, *Eur. J. Cancer* **26**: 101-106.
- Marquardt D and Center MS (1991) Involvement of vacuolar H^{+} -Adenosine triphosphatase activity in multidrug resistance in HL60 cells, *J. Nat. Cancer Inst* **83**: 1098-1102.
- Mason RP, Cha GH, Gorrie GH, Babcock EE and Antich PP (1993) Glutathione in whole blood: a novel determination using double quantum coherence transfer proton NMR spectroscopy, *FEBS Lett.* **318**: 30-34.
- Roepe PD, Wei LY, Cruz J and Carlson D (1993) Lower electrical membrane potential and altered pH_i homeostasis in multidrug-resistant (MDR) cells: further characterization of a series of MDR cell lines expressing different levels of P-glycoprotein, *Biochemistry* **32**: 11042-56.
- Sehested M, Skovsgaard T, van Deurs B, and Winther-Neilson H (1987) Increased plasma membrane traffic in daunorubicin resistant P388 leukemic cells: effect of daunorubicin and verapamil, *Br. J. Cancer* **56**: 747-751.

Sehested M, Skovsgaard T and Roed H (1988) The carboxylic ionophore monensin inhibits active drug efflux and modulates in vitro resistance in daunorubicin resistant Ehrlich ascites tumor cells, *Biochem. Pharmacol.* **37**: 3305-3310.

Simon S, Roy D and Schindler M (1994) Intracellular pH and the control of multidrug resistance, *Proc. Nat. Acad. Sci. USA* **91**: 1128-1132.

Tannock IF and Rotin D (1989) Acid pH in tumors and its potential for therapeutic exploitation, *Cancer Res.* **49**: 4373-84.

Taylor CW, Dalton WS, Parrish PR, Gleason MC, Bellany WT, Thompson FH, Roe DJ and Trent JM (1991) Different mechanisms of decreased drug accumulation in doxorubicin and mitoxantrone resistant variants of the MCF7 human breast cancer cell line, *Br. J. Cancer* **63**: 923-929.

Thiebaut F, Currier SJ, Whitaker J, Haugland RP, Gottesman MM, Pastan I and Willingham MC (1990) Activity of the multidrug transporter results in alkalinization of the cytosol: measurement of cytosolic pH by microinjection of a pH-sensitive dye, *J. Histochem. Cytochem.* **38**: 685-90.

Willingham MC, Cornwell MM, Cardarelli CO, Gottesman MM and Pastan I (1986) Single cell analysis of daunomycin uptake and efflux in multidrug-resistant and -sensitive KB cells: effects of verapamil and other drugs, *Canc. Res.* **46**: 5941-5946.